PBPK Model for Atrazine and Its Chlorotriazine Metabolites in Rat and Human

Jerry L. Campbell Jr.,*,[1] Melvin E. Andersen,* Paul M. Hinderliter,[†]
Kun Don Yi,[†] Timothy P. Pastoor,[‡] Charles B. Breckenridge,[†] and
Harvey J. Clewell III*

*The Hamner Institutes for Health Sciences, Center for Human Health Assessment, Research Triangle Park,
North Carolina 27709-2137; [†]Syngenta Crop Protection, LLC, Greensboro, North Carolina 27419-8300; and
[‡]Pastoor Science Communications, LLC, Greensboro, North Carolina 27455-3415

[1]To whom correspondence should be addressed at The Hammer Institute for Health Sciences, 6 Davis Drive, P.O. Box 12137, Research Triangle Park, NC
27709-2137. Fax: 919-558-1300. E-mail: jcampbell@ramboll.com.

ABSTRACT

The previously-published physiologically based pharmacokinetic model for atrazine (ATZ), deisopropylatrazine (DIA), deethylatrazine (DEA), and diaminochlorotriazine (DACT), which collectively comprise the total chlorotriazines (TCT) as represented in this study, was modified to allow for scaling to humans. Changes included replacing the fixed dose-dependent oral uptake rates with a method that represented delayed absorption observed in rats administered ATZ as a bolus dose suspended in a methylcellulose vehicle. Rate constants for metabolism of ATZ to DIA and DEA, followed by metabolism of DIA and DEA to DACT were predicted using a compartmental model describing the metabolism of the chlorotriazines by rat and human hepatocytes *in vitro*. Overall, the model successfully predicted both the 4-day plasma time-course data in rats administered ATZ by bolus dose (3, 10, and 50 mg/kg/day) or in the diet (30, 100, or 500 ppm). Simulated continuous daily exposure of a 55-kg adult female to ATZ at a dose of 1.0 µg/kg/day resulted in steady-state urinary concentrations of 0.6, 1.4, 2.5, and 6.0 µg/L for DEA, DIA, DACT, and TCT, respectively. The TCT (ATZ + DEA + DIA + DACT) human urinary biomonitoring equivalent concentration following continuous exposure to ATZ at the chronic point of departure (POD = 1.8 mg/kg/day) was 360.6 µg/L.

Key words: atrazine; chlorotriazines; pharmacokinetics; metabolism PBPK model; risk assessment.

Atrazine (ATZ) is used to control broadleaf and some grassy weeds in corn, sorghum, and sugar cane (Bridges, 2008). ATZ and its chlorotriazine metabolites, deisopropylatrazine (DIA), deethylatrazine (DEA), and diaminochlorotriazine (DACT), are detected in drinking water in the United States, predominantly in the Midwest during the spring planting season (Breckenridge *et al.*, 2016; Tierney *et al.*, 2008). The 12-month rolling-average, maximum contaminant level for ATZ in drinking water has been set by the United States Environmental Protection Agency (USEPA) at 3 µg/L. A 90-day rolling-average concentration of 12.5 µg/L has been established for the chlorotriazines, based on EPA's conclusion that the chlorotriazines (ATZ, simazine, and propazine) and their chlorotriazine metabolites (DEA, DIA, and DACT) share a common mechanism of toxicity (USEPA, 2002).

Administration of ATZ to young adult, female Sprague Dawley (SD) rats, by gavage at a dose of 50 mg/kg/day for 4 days, resulted in the suppression of the luteinizing hormone (LH) surge and a reduction in the number of ova that were released. There were no effects on either the LH surge or ovulation when the same dose was given as a temporally distributed dose in feed (Foradori *et al.*, 2014). High bolus doses of ATZ also reduced LH pulse frequency (Foradori *et al.*, 2013), an effect that has been linked to delayed onset of puberty (Breckenridge *et al.*, 2015), as observed in both male (Stoker *et al.*, 2000) and female rats (Ashby *et al.*, 2002; Laws *et al.*, 2000, 2003). The

no-observable-adverse-effect levels (NOAELs) for ATZ's effect on puberty (NOAEL = 6.25 mg/kg/day) and the LH surge (NOAEL = 1.8 mg/kg/day) are used to set 30-day (NOAEL = 6.25 mg/kg/day), 90-day (NOAEL = 1.8 mg/kg/day), and lifetime (NOAEL = 1.8 mg/kg/day) points of departure (PODs) for ATZ and its chlorometabolites (USEPA, 2006).

The magnitude, frequency, and duration of exposure to chlorotriazines are important determinants of whether adverse effects are observed in animal models (Breckenridge *et al.*, 2015; Foradori *et al.*, 2014). This article describes a physiologically based pharmacokinetic (PBPK) model that is capable of converting time-varying concentrations of ATZ, DEA, DIA, and DACT in drinking water into estimates of internal human plasma concentrations for each chemical separately and for calculating total chlorotriazines (TCT) plasma concentrations. Because human exposure is often reported as concentrations of chlorotriazines in urine, we used the PBPK model to calculate the human biomonitoring equivalent (BE) urinary concentrations of DEA, DIA, and DACT at a steady-state exposure to ATZ at a dose of 1.0 μg/kg/day. The BE urinary concentration estimates for the chlorotriazines, provided in this study, will facilitate the interpretation of human urinary biomonitoring data (Barr *et al.*, 2007), and assist in determining whether associations reported in observational epidemiology studies on the chlorotriazines (Chevrier *et al.*, 2011, 2014; Goodman *et al.*, 2014) are biologically plausible (Adami *et al.*, 2011).

The previously published PBPK model for ATZ, DEA, DIA, and DACT (McMullin *et al.*, 2007a, b) could not be used to extrapolate doses from rodents to humans. This was because it relied on a fixed function to characterize oral dose uptake that was specific to the method of administration. In this revised model, rate constants for the conversion of ATZ to DEA, DIA, and DACT were based on new *in vitro* metabolism studies conducted on rat and human hepatocytes. The dose-dependent absorption function used by McMullin *et al.* (2007b) was replaced with a description that defines the solubility of ATZ in the aqueous, methylcellulose suspension typically used in rodent studies. Validation of the re-derived PBPK model was evaluated by comparing predicted plasma concentrations in rats to measure plasma concentrations after 4 daily doses of ATZ, administered either as bolus doses of 3, 10, or 50 mg/kg/day or as a temporally distributed dose in diet at concentrations of 30, 100, or 500 ppm.

The elimination of DEA, DIA, and DACT from plasma was used to estimate urinary elimination of these chlorometabolites in humans. Model-predicted elimination of DEA, DIA, and DACT in human urine was compared with results obtained from a human study conducted by Davidson (Pfeil *et al.*, 2007). In a second study (Breckenridge *et al.*, 2016), model-predicted human plasma TCT concentrations were calculated every 15 min for subpopulations of individuals who were simulated to be exposed to ATZ and its chlorometabolites in drinking water. Daily average peak plasma TCT and area under the curve (AUC) TCT concentrations following simulated exposure were determined. Margins of exposure (MOEs) were calculated as ratios of the predicted plasma TCT concentrations to plasma TCT concentrations for a number of toxicological PODs.

MATERIALS AND METHODS

Overview of Modeling Approach

Revisions of the chlorotriazine PBPK model (Figure 1) and the Advanced Computer Simulation Language (ACSL) code (Supplementary Appendix 1), initially developed by McMullin *et al.* (2007b) were based on new *in vitro* metabolism data from studies in rat (Figs. 2 and 3) and human hepatocytes (Figure 4), new pharmacokinetic data in the female SD rats (Figs. 5 and 6), and information on human urinary clearance of the chlorotriazines (Pfeil *et al.*, 2007). Additional compartments, not shown in Figure 1, were included in the revised model (see Table 1, and Supplementary Appendix 1). Physiological parameters used in the model (Table 1) were obtained from the published literature (Brown *et al.*, 1997; O'Flaherty *et al.*, 1992). Blood perfusion of tissues was described as flow limited. Human tissue volumes and blood flow rates (Table 1) were obtained from the published literature (ICRP, 2002). Physiological parameters that were unavailable in the published literature for the rat were estimated by using human parameters, adjusted for body weight. Tissue-to-blood partition coefficients were assumed to be 0.7 for the parent molecule, ATZ, as well as for DEA, DIA, and DACT. This is consistent with partition coefficients reported by Tremblay *et al.* (2012) for ATZ.

In Vitro Hepatocyte Studies

The oxidative metabolism of ATZ in the liver to DIA, DEA, and DACT (Figure 7) is described as a saturable process. Competitive inhibition (ie, ATZ metabolism inhibited by DIA and DEA; DIA metabolism inhibited by ATZ and DEA; and DEA metabolism inhibited by ATZ and DIA), which was originally described by McMullin *et al.* (2007b), was also incorporated into the revised model. The processes of chlorotriazine conjugation with glutathione and conversion to mercapturates (Figure 7) are not in the current model because direct estimates of the rate constants for these reactions were not available. These metabolites, which were rapidly eliminated into the urine of non-human primates dosed with ATZ (unpublished data), are not detectable in plasma and do not contribute to the toxicity of the chlorotriazines.

The *in vitro* oxidative metabolism rates for ATZ to DEA, DIA, and DACT were determined in rat and human hepatocytes (McMullin *et al.*, 2007a). McMullin *et al.* incubated intact rat hepatocytes with ATZ for 90 min at initial concentrations of 1.74, 44, 98, or 266 μM and measured changes in the concentration of the chlorometabolites over time. In a new study, rat or human hepatocytes (0.5 × 10^{6} hepatocytes per mL media) were incubated with ATZ at nominal concentrations of 0.5, 1.0, or 1.7 μM, and average initial concentrations of 0.45, 1.26, or 1.43 μM in rat hepatocytes and 0.42, 1.38, or 1.43 μM in human hepatocytes, respectively. The concentrations of ATZ, DEA, DIA, and DACT in the incubation media were assessed by HPLC at 0, 5, 10, 20, 30, 45, 60, 90, 120, 180, and 240 min after exposure initiation. The *in vitro* concentrations measured after time 0 were adjusted for slight decreases in cell viability observed over the incubation period.

The time-course concentration profiles of ATZ, DIA, DEA, and DACT in incubation media with intact rat or human hepatocyte suspensions were modeled by using 4 differential equations to characterize (1) the rate of metabolism of ATZ; (2) the rate of formation of DIA and DEA from ATZ; and (3) the rate of formation of DACT from DIA and DEA (McMullin *et al.*, 2007a) (Figure 7). To account for the reduced conversion rates to DACT observed at higher incubation concentrations, competitive inhibition information between substrates for ATZ, DIA, and DEA was included in the model.

Michaelis–Menten affinity constants (K_m) for ATZ, DEA, and DIA were 30, 13, and 13 μm, respectively (McMullin *et al.*, 2007a). Maximum metabolism rates (V_{max}) were estimated serially; then the fraction of either DIA or DEA produced from ATZ was estimated. V_{max}s for ATZ, DIA, and DEA were determined. V_{max} for
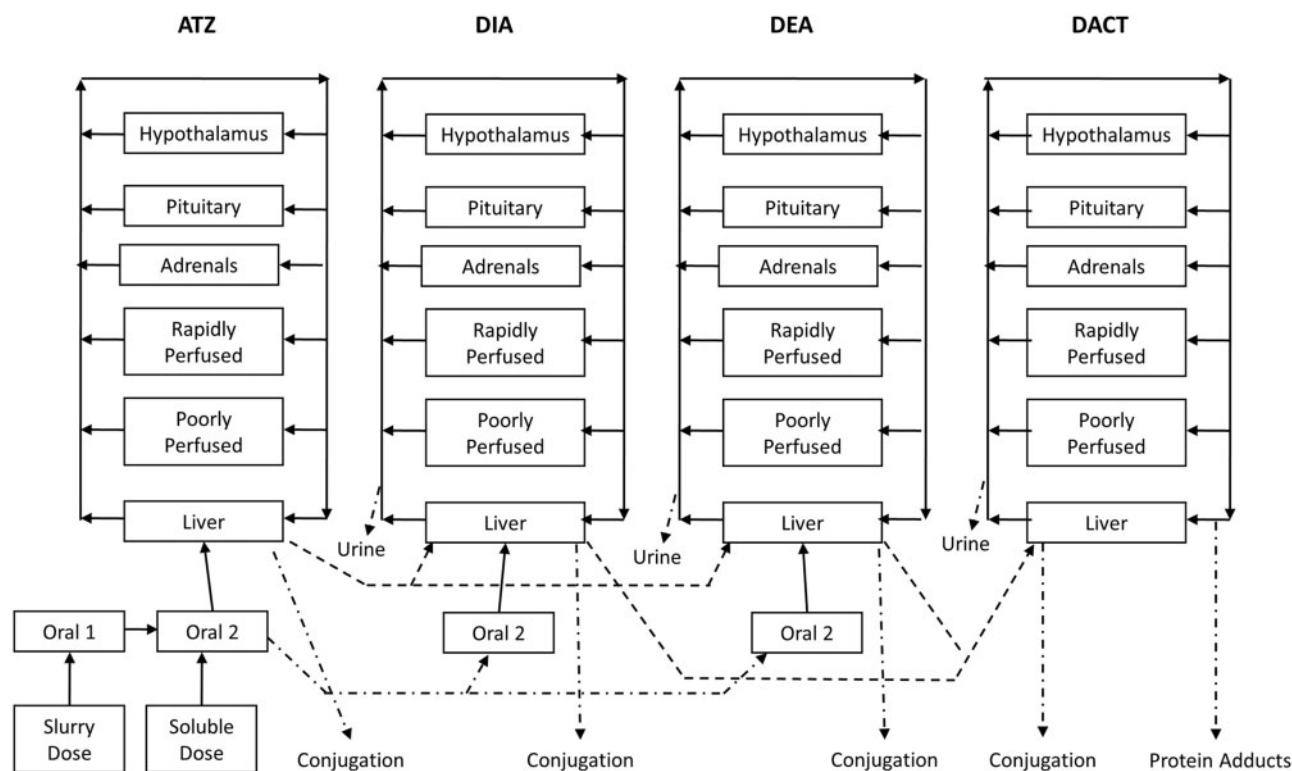
FIG. 1. Schematic of the PBPK model for ATZ and the chlorotriazine metabolites (dashed lines represent clearance of ATZ, DIA, DEA, and DACT through either sequential metabolism, conjugation with thiol, protein adduction, or urinary excretion).

DACT was defined as the sum of the rates of metabolism of DIA and DEA. A first-order elimination rate constant was added to the *in vitro* metabolism model for DACT to account for measured loss of DACT from the media at the end of the incubation period.

Estimated parameters for the saturable metabolism of ATZ, DIA, and DEA *in vitro* were scaled to the whole animal based on hepatocellularity of the liver, as described by Sohlenius-Sternbeck (2006). The number of hepatocytes per gram was predicted from protein-based analysis, with the number of cells per gram of liver reported as 117×10^6 for rat and 139×10^6 for human. V_{maxs} estimated from the *in vitro* hepatocyte suspension assays (Table 2) were scaled to rat and human whole body values using Equation 1.

$$V_{max(whole\ body)} = \frac{V_{hepatocytes} \times \text{Total number of hepatocytes}}{\text{Body weight}^{3/4}}.$$

(1)

The resulting rate constants were used in the PBPK model; the units were expressed as $\mu mol/h/kg\ BW^{0.75}$ (Table 3).

In Vivo Rat Studies

Several studies have characterized the *in vivo* pharmacokinetics of ATZ after oral gavage dosing. In one study, ^{14}[C]-ATZ was administered by oral gavage to female SD rats daily for 7 days at doses of 1, 3, 7, 10, 50, or 100 mg ATZ/kg. Plasma concentrations of ^{14}[C]-ATZ were measured 24 h after each daily dose, and also daily during a 3-day washout period (Thede, 1987). In a second study (Timchalk *et al.*, 1990), total ^{14}[C]-ATZ equivalent plasma concentration was evaluated for up to 80 h after a single oral dose of 30 mg radiolabeled ^{14}[C]-ATZ per kg of body weight. In another study (McMullin *et al.*, 2007a, b), rats were administered

ATZ by gavage at a dose of 150 mg/kg and plasma samples were collected for up to 70 h post-dosing.

New time-series plasma concentration data for ATZ, DEA, DIA, and DACT, during and after 4 daily oral gavage doses of 3, 10, or 50 mg/kg ATZ/day, are shown in Figure 5. The comparable data obtained after administration of ATZ in diet at concentrations of 30, 100, or 500 ppm are provided in Figure 6. Plasma concentrations of ATZ and its chlorometabolites were also evaluated during a 4-day washout period. The average daily dietary doses, which were determined on the basis of the amount of food consumed during the light (10-h) and dark (14-h) photoperiods, were 3, 9, and 43 mg/kg/day, in the 30, 100, and 500 ppm groups, respectively. The diurnal variation in food consumption was taken into account when predicting internal plasma concentrations of ATZ and its chlorometabolites after dietary exposure.

Model Calibration

Absorption
A 2-compartment, empirical model was used to fit the oral uptake of ATZ (Figure 1). One compartment represented insoluble ATZ non-covalently bound to methylcellulose or food, and the other compartment represented free ATZ in solution. To simulate the uptake of ATZ from the gut, it was assumed that ATZ initially resided in the Oral 1 (bound) compartment and became available for absorption at a rate specified in $\mu mol/kg/h$. A first-order rate constant was used to describe the release of bound ATZ from Oral 1. Metabolism of free ATZ was described as a first-order process. No pre-systemic metabolism of DIA and DEA was included the model. The model assumed that all free ATZ, DIA, and DEA chlorotriazines are absorbed.
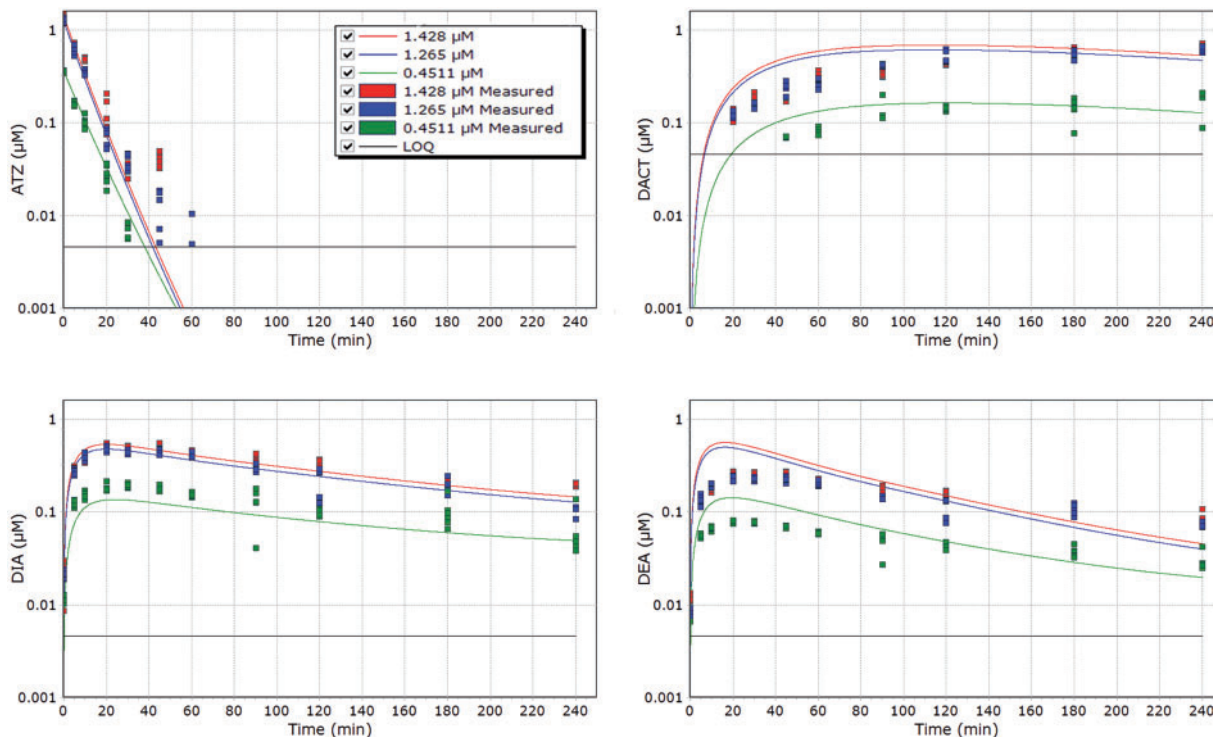
FIG. 2. Model prediction of intact rat hepatocyte metabolic assays for ATZ and its chlorinated metabolites (0.25 mL incubations with 0.5 × 106 cells per well; initial concentrations were 1.43 μM—Group 1, 1.26 μM—Group 2, and 0.45 μM—Group 3).
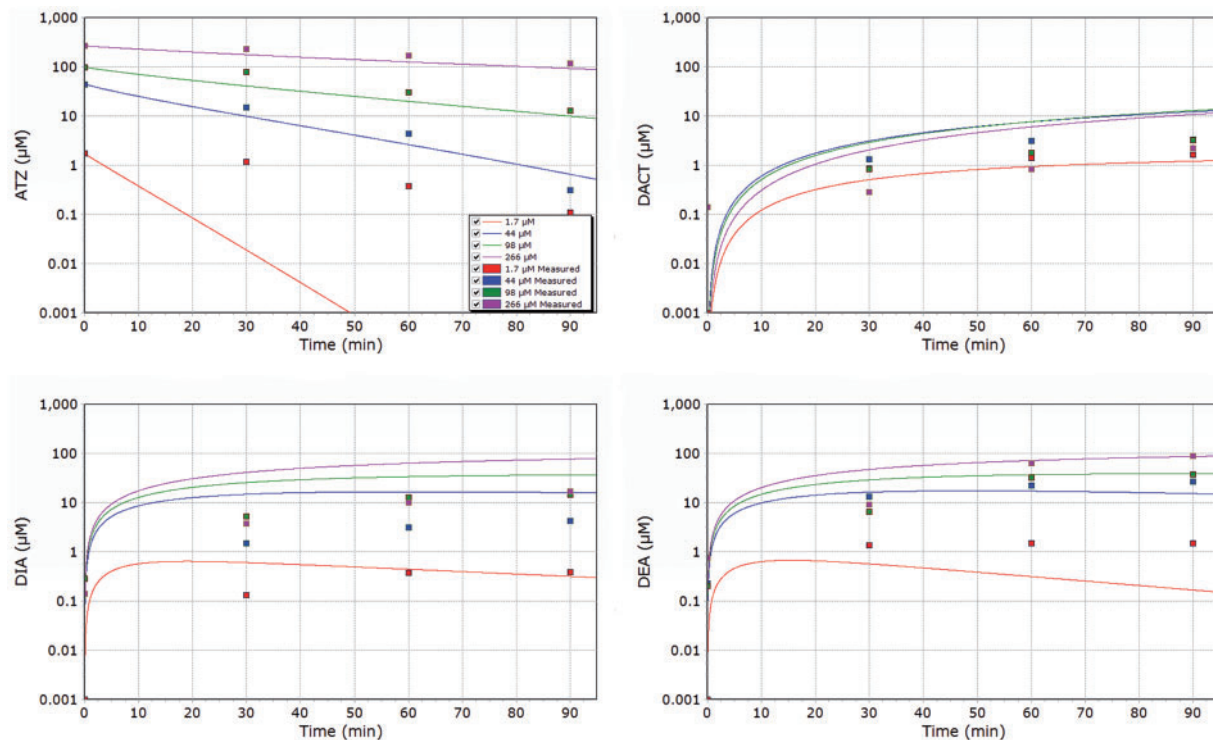

FIG. 3. Model prediction of intact rat hepatocyte metabolic assays for ATZ and its chlorinated metabolites (McMullin *et al.*, 2007b).
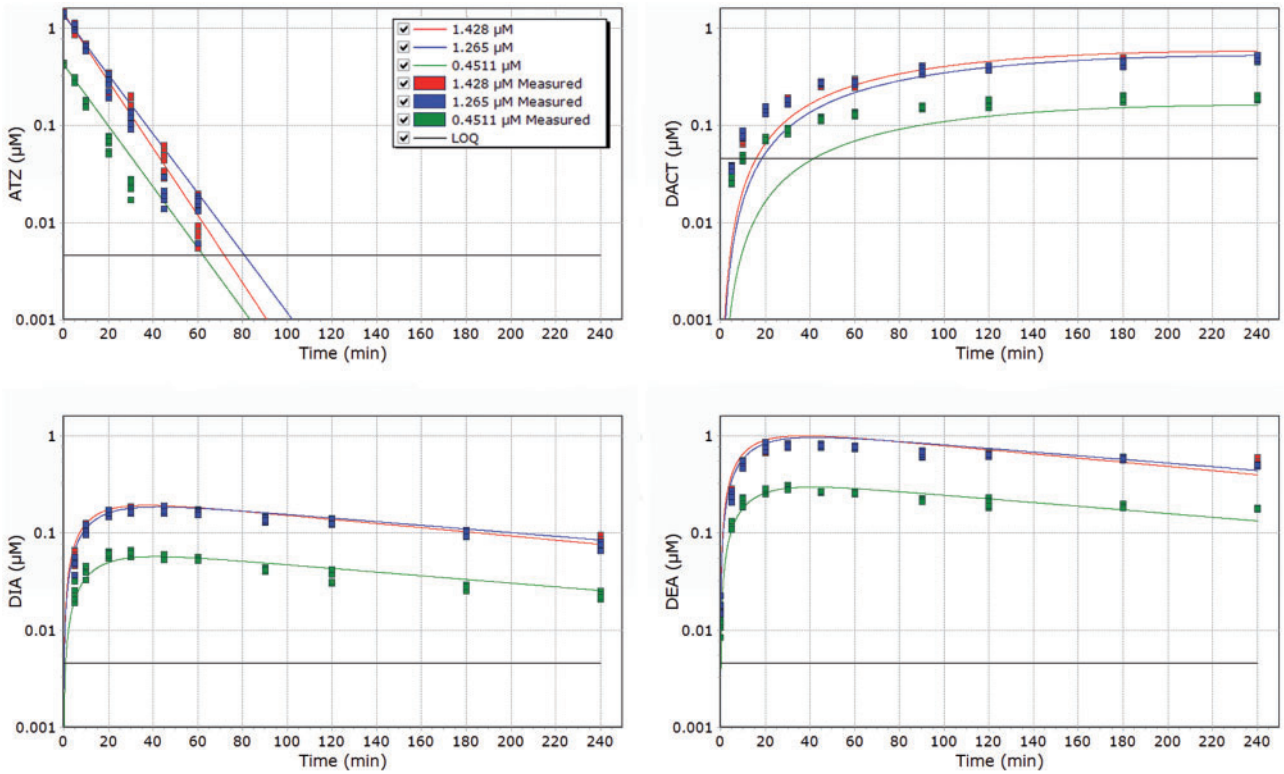
FIG. 4. Model prediction of intact human hepatocyte metabolic assays for ATZ and its chlorinated metabolites (0.25 mL incubations with 0.5 × 10⁶ cells per well; initial concentrations were 1.43 μM—Group 1, 1.38 μM—Group 2, and 0.42 μM—Group 3).
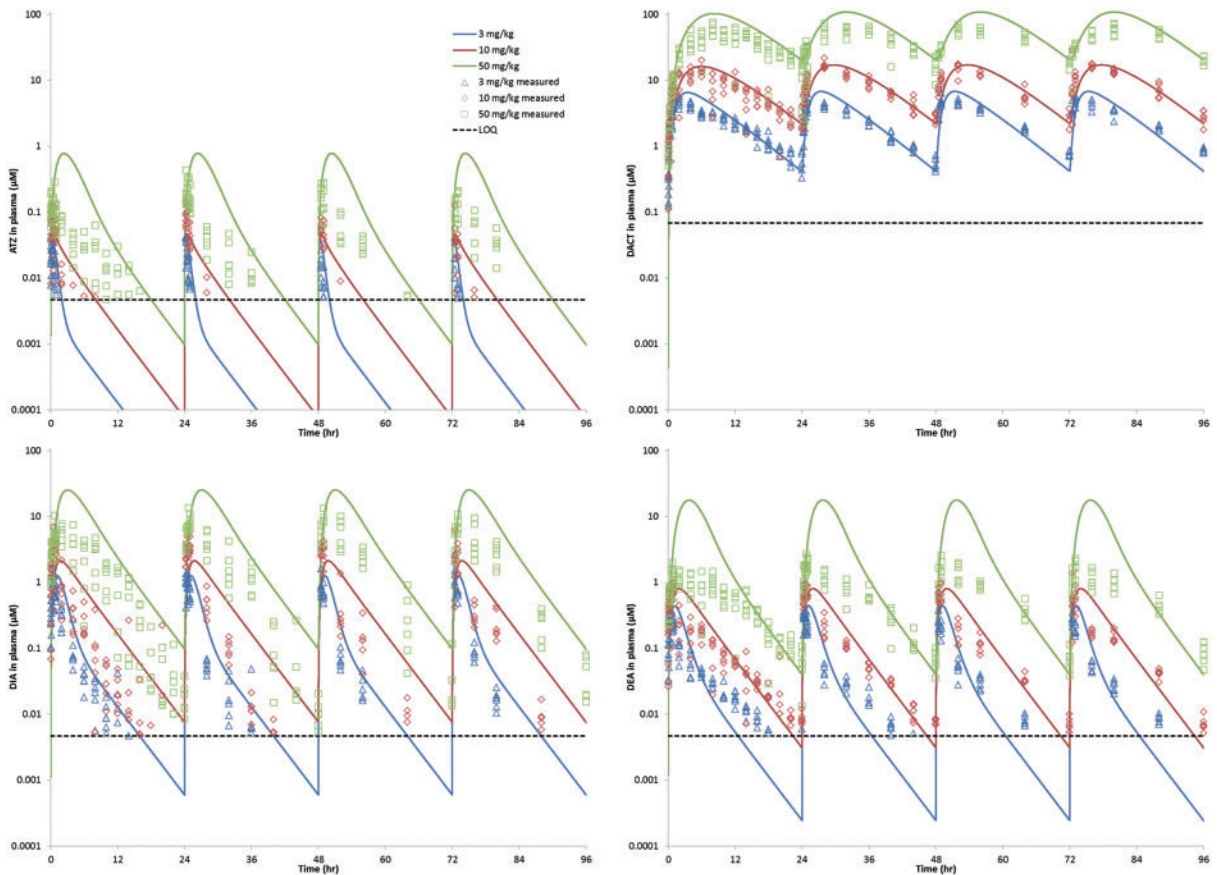

FIG. 5. Model predictions of ATZ and chlorinated metabolites during and after repeated daily gavage doses of ATZ at 3, 10, and 50 mg/kg. Four oral gavage doses were administered at 0, 24, 48, and 72 h with sampling out to 192 h. Symbols represent individual animal plasma samples. Solid lines represent corresponding model simulations.
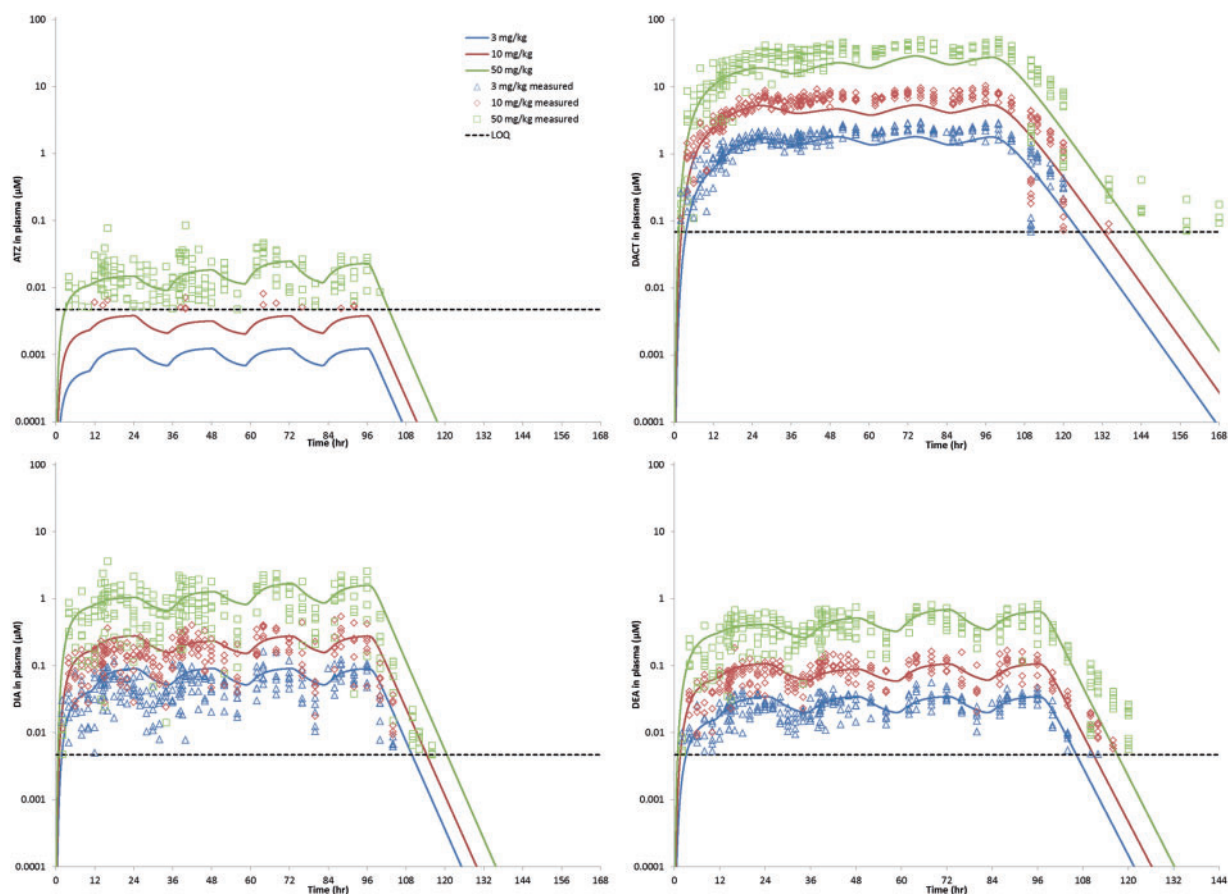
FIG. 6. Model predictions of ATZ and chlorinated metabolites during and after repeated dietary exposure to ATZ at 3, 10, and 50 mg/kg. ATZ administered continuously in the diet (3, 10, or 500 ppm) for 96 h with sampling out to 192 h. Symbols represent individual animal plasma samples. Solid lines represent corresponding model simulations.

Rate constants for the oral uptake and metabolism of ATZ are provided in Table 3. These rate constants (ie, uptake; transport from the slow to the fast oral compartment [Oral 1 to Oral 2]; gut metabolism of ATZ; the Oral 2 fraction; and estimates of the insoluble portion of the dose) were all fit to provide the best description of the appearance of ATZ, DIA, and DEA in plasma from the single oral gavage dose data (Figure 5).

Elimination
Since urinary elimination of ATZ or its chlorometabolites was not measured in any of the *in vivo* rat studies, the rate of elimination of the chlorotriazine in urine was assumed to be directly proportional to the rate of clearance from plasma. Studies have shown that a small fraction of DACT in plasma is dechlorinated and covalently bound through a free thiol-linkage onto cysteine residue 34 of rat and human albumin (Dooley *et al.*, 2007). To simulate the terminal clearance of total radioactivity from rat plasma, a rate of reaction with albumin was estimated to provide sufficient albumin-bound ^{14}C-ATZ equivalents in plasma (Timchalk *et al.*, 1990), with the terminal clearance time based on the turnover of serum albumin in rats. The elimination rate constant for albumin was set equivalent to the half-life of albumin in blood for the rat ($\approx$46 h), as described in McMullin *et al.* (2003). Although DACT is known to adduct to human plasma albumin, the small amount eliminated via protein adduction in humans was accounted for in the estimation of the overall reaction rate (ie, KELIMDAC), which describes the difference

between the loss of DACT from plasma and the appearance of DACT in urine in the human study.

The urinary concentrations of ATZ, DEA, DIA, and DACT were measured daily for 7 days (24-h voids) in 6 human volunteers that were administered a single oral dose of 0.1 mg ATZ per kg body weight. Since ATZ was below the limit of quantification (LOQ) in all urine samples (Pfeil *et al.*, 2007), rate constants for the urinary elimination of DIA, DEA, and DACT were calculated and compared with PBPK-predicted values based on clearance of these metabolites from plasma, and then scaled from rodent to man.

The elimination rate constants for ATZ, DIA, DEA, and DACT, which represent chemical reactions with thiols, including the thiol on glutathione (Figure 7) (Jablonkai and Hatzios, 1993), were adjusted on the basis of the concentrations of ATZ and the chlorinated metabolites in plasma time-course data for rats. Similar adjustments were made to the plasma and urinary excretion data for humans (Figure 8).

RESULTS

In Vitro Performance of the Model

Overall, the *in vitro* concentrations of ATZ, DEA, DIA, and DACT in intact rat hepatocytes were adequately predicted by the model (Figs. 2 and 3). The model provided a better description of the high-concentration data (Groups 1 and 2; Figure 2) and the

TABLE 1. Physiological Parameters for the ATZ PBPK Model

Physiological parameters	Symbol	Rat	Human
Body weight(kg)	BW	0.25	60
Fraction of Body Weight			
Liver	VLC	0.034[a]	0.026[a]
Brain	VBRC	0.006[a]	0.02[a]
Pituitary	VPITC	0.00001	0.0000082[b]
Hypothalamus	VHTLC	0.0000104	0.000014[c]
Fat	VFC	0.07[a]	0.21[a]
Mammary	VMAC	0.01	0.00034[b]
Testes/Ovaries	VROC	0.0063	0.00048[b]
Adrenal	VADC	0.0002	0.0002
Rapidly Perfused	VRPC	0.25-VLC-VBRC-VHTLC	0.25-VLC-VBRC-VHTLC
Poorly Perfused	VSPC	0.91-Sum other tissue Fractions	0.91-Sum other tissue Fractions
Blood	VBLC	0.074[a]	0.079[a]
Cardiac output (L/hr/kg$^{0.74}$)	QCC	18.7	15.6
Fraction of QC			
Liver	QLC	0.174	0.25
Brain	QBRC	0.02	0.114
Pituitary	QPITC	0.00000273	0.0000467
Hypothalamus	QHTLC	0.0000483	0.0000827
Fat	QFC	0.07	0.05
Mammary	QMAC	0.0002	0.0002
Testes/Ovaries	QROC	0.0005	0.0012
Adrenal	QADC	0.003	0.003
Poorly Perfused	QSPC	0.19	0.19
Rapidly Perfused	QRPC	1–sum other tissue fractions	1–sum other tissue fractions

[a]Brown et al. (1997).
[a]Brown et al. (1997).
[b]ICRP (2002).
[c]Koolschijn et al. (2008).

data for concentrations of 44 μM and above from McMullin *et al.* (2007a). The model over-predicted the rate of disappearance of ATZ for the 1.7 μM concentration group from McMullin *et al.* (2007a). The source of the difference is due to the fact that the McMullin et al. (2007a) estimate of the maximum rate of enzymatic conversion of ATZ to DEA and DIA together in rodent hepatocytes (Figure 3) was ~10-fold slower than observed in our recent studies (Figure 2). Thus, in our study on rat hepatocytes, ATZ rapidly disappeared from the media (approximately a 50% reduction by 5 min), whereas in McMullin *et al.* (2007a), it took ~10 times longer (~50 min) to achieve a similar decline. The basis of this difference between studies is unknown, but we have confidence in our new data because the results were replicated at 3 ATZ concentrations that were selected because they fell within a plausible, physiological range.

Parameters estimated from the rat *in vitro* studies were used as the starting point to estimate the fraction and the maximum velocities for ATZ, DIA, and DEA for the human. Initially, it was assumed that affinity constants were the same in both species. Minimal adjustments were required to provide acceptable fit of model predictions to the human hepatocyte *in vitro* data (Figure 4). Human hepatocytes, however, preferentially converted ATZ to DEA instead of DIA, whereas rat hepatocytes preferentially converted ATZ to DIA. The overall rate of clearance of ATZ from the suspension media was comparable in the rat and human hepatocyte cultures, as was the rate of formation of DACT.

In Vivo Performance of the Model

Model predictions of the repeated oral bolus and dietary exposure data are shown in Figures 5 and 6. The rate constants derived from the *in vitro* hepatocyte assay, scaled to the whole animal, provided a good fit of the 4-day, repeated oral bolus, time-course data for ATZ doses of 3 and 10 mg/kg. In the 50 mg/kg/day dose group, the model tended to over-predict the peak plasma concentrations for all 4 chlorotriazines. Given that the model predictions fit the DACT plasma time-course data well at 50 mg/kg and the ATZ, DIA, and DEA plasma time course data at 3 and 10 mg/kg, the structure of the oral absorption compartment was not altered to improve model predictions of the 50 mg/kg time-course data.

For the dietary study, model-predictions fit the empirical data very well (Figure 6). The model provided a good characterization of the slow increase to pseudo-steady-state concentrations of DACT. Model predictions of initial clearance following withdrawal from exposure were also acceptable. While the terminal phase of the clearance was over-predicted, almost all of this data were at or below the LOQ for the analytical methods.

Human Parameterization

The human model was parameterized using methods similar to those employed in the rat model. Human physiological parameters (Table 1) were obtained from the published literature (Brown *et al.*, 1997; ICRP, 2002). The metabolic rate constants for liver were estimated from the *in vitro* hepatocyte suspension studies, as described previously. The oral absorption rate constants, derived from rats, were scaled to humans. These absorption rate estimates were sufficient to adequately describe the available human data (Figure 9).
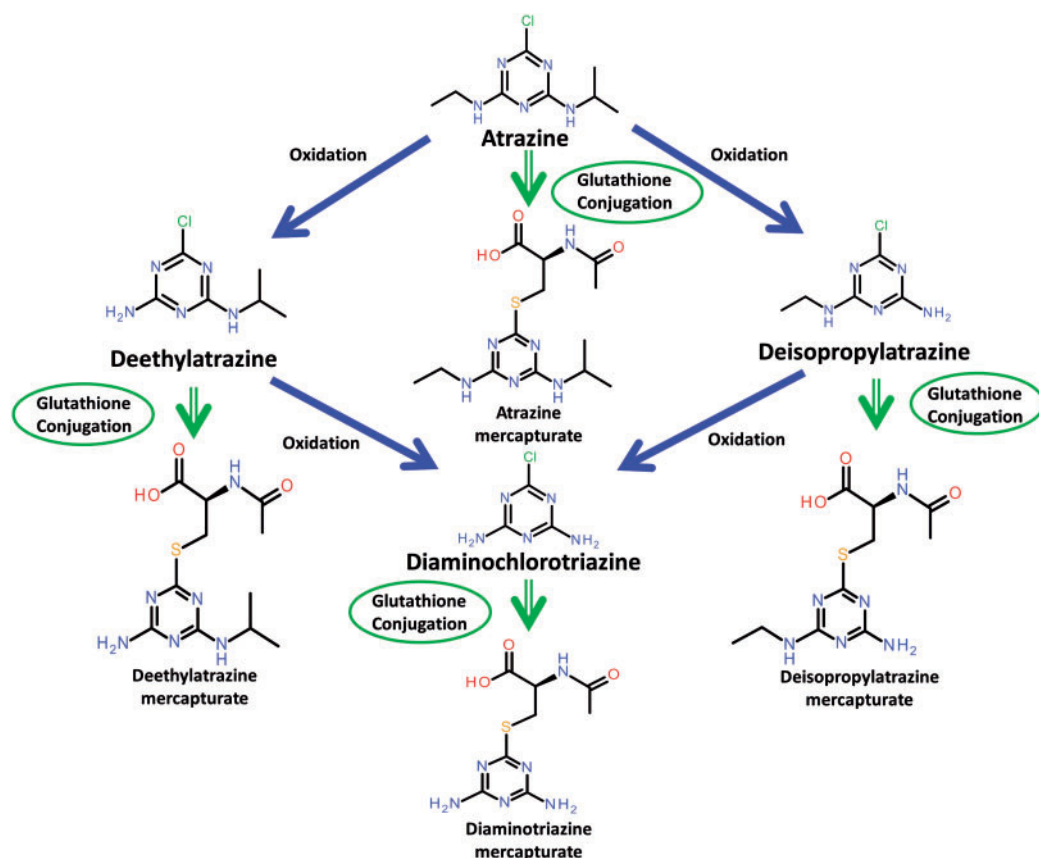
FIG. 7. Schematic representation of major Phases 1 and 2 metabolites of ATZ, DEA, DIA, and DACT.

TABLE 2. Parameters Used to Simulate the *In Vitro* Intact Hepatocyte Metabolism of ATZ and Its Chlorinated Metabolites

Parameter	Symbol	Species	
		Rat	Human
Volume of hepatocyte suspension (mL)	VSUSP	0.25	0.25
Initial number of hepatocytes (10^6)	INITNOHEPAT	0.5	0.5
ATZ			
V_{max} (μmol/10^6 cells/min)			
ATZ to DIA	VMAXCATRAI	0.0012	0.00025
ATZ to DEA	VMAXCATRAE	0.0014	0.0013
Affinity constant ATZ (μM)	KMATRA	30.0	30.0
DIA			
V_{max} (μmol/10^6 cells/min)	VMAXCISO	0.00008	0.00004
Affinity constant DIA (μM)	KMISO	13.0	13.0
DEA			
V_{max} (μmol/min/10^6 hepatocytes)	VMAXCETHYL	0.00015	0.00004
Affinity constant DEA (μM)	KMETHYL	13.0	13.0
DACT			
Clearance (mL/min)	KELDACT	0.0000013	0.000001

Performance Compared to Human Data

The PBPK model under-predicted the measured peak plasma concentration of DEA by a factor of 3 for data from a single human volunteer (Figure 9A, top), and slightly over-predicted the peak DACT concentration (within a factor of 2). The model provided an excellent fit of the cumulative urinary excretion data for DIA, DEA, and DACT in 6 subjects (Figure 9, bottom).

Sensitivity

A sensitivity analysis of the adult human ATZ PBPK model was conducted using the same scenario described for the derivation of the BE. Normalized sensitivity coefficients were calculated using the forward-difference method for all chemical specific parameters in the model, the oral uptake rate constants, the elimination rate constants, and the partition coefficients.

TABLE 3. Oral Uptake and Metabolic Parameters for ATZ, DIA, DEA, and DACT

| Oral absorption parameters	Units	Symbol	Rat	Human
Insoluble portion of oral dose	mg/kg	DOINSOL	2400	–
ATZ Absorption rate in Oral 2	/h*BW$^{0.25}$	KADUOATRAC	0.09	0.09
ATZ Transfer rate: Oral 1 to Oral 2	/h*BW$^{0.25}$	KSTDUOATRAC	0.181	0.181
ATZ Metabolism to DIA in Oral 2	/h*BW$^{0.25}$	KMETATRA_ISO_OR2C	0.917	1.05
ATZ Metabolism to DEA in Oral 2	/h*BW$^{0.25}$	KMETATRA_ETHYL_OR2C	0.393	0.26
DIA Absorption rate in Oral 2	/h*BW$^{0.25}$	KADUOISOC	0.8	0.8
DEA Absorption rate in Oral 2	/h*BW$^{0.25}$	KADUOETHYLC	0.6	0.6
DACT Absorption rate in Oral 2	/h*BW$^{0.25}$	KADUODAC	0.6	0.6
Metabolism/clearance parameters				
ATZ Elimination	L/h-kg Liver	KELIMATRAC	41.01	41.01
ATZ to DIA: Maximum velocity in liver	μmol/h/BW$^{0.75}$	VMAXCATRAI	202.5	188.2
ATZ to DEA: Maximum velocity in liver	μmol/h/BW$^{0.75}$	VMAXCATRAE	236.3	752.6
ATZ Affinity constant	μmol/L	KMATRA	30.0	30.0
DIA Elimination	L/h-kg Liver	KELIMISOC	48.4	48.4
DIA to DACT: Maximum velocity in liver	μmol/h/BW$^{0.75}$	VMAXCISO	13.5	25.1
DIA Affinity constant	μmol/L	KMISO	13.0	13.0
DEA Elimination	L/h-kg Liver	KELIMETHYLC	7.07	7.07
DEA to DACT: Maximum velocity in liver	μmol/h/BW$^{0.75}$	VMAXCETHYL	25.3	25.1
DEA Affinity constant	μmol/L	KMETHYL	13.0	13.0
Covalent binding of DACT	/h*BW$^{0.25}$	KDAALBC	0.016	–
Turnover of serum albumin	/h*BW$^{0.25}$	KALBC	0.01	–
Elimination of DACT	L/h-kg Liver	KELIMDAC	1.191	20.6
Urinary clearance				
DIA	L/h*BW	CLRISOC	0.0016	0.2
DEA	L/h*BW	CLRDEAC	0.0053	0.2
DACT	L/h*BW	CLRDAC	0.0521	0.069
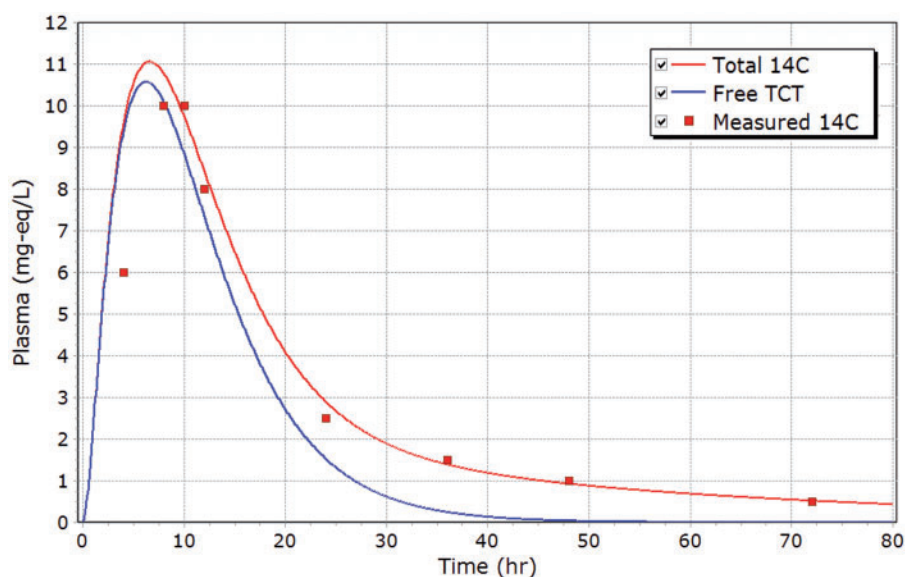
FIG. 8. Simulation of the plasma time-course total chlorotriazine concentration in rat following a single oral gavage dose of 30 mg radiolabeled ^{14}[C]-ATZ/kg body weight (points are means taken from Timchalk et al., 1990). The red line includes the amount of labeled triazine ring-bound to plasma protein along with total chlorotriazines, while the blue line represents only the total labeled chlorotriazines.

Changes in the plasma and urinary concentration of ATZ, DEA, DIA, DACT, and TCT were calculated after making a 1% change in each model parameter. A parameter was deemed sensitive if the resulting coefficient was ≥0.1. Sensitivity coefficients, calculated for all rate constants and partition coefficients, are provided in Table 4. Only those parameters that affected at least 1 response variable are shown. In general, the average concentration of ATZ

and its metabolites in plasma and urine was sensitive to the rate constants for metabolism or clearance of each specific chlorotriazine. Average concentrations of DACT in plasma, and to a greater extent in urine, were sensitive to V_{max} and K_m for metabolism of DEA to DACT. DACT concentration in urine, however, was more sensitive to DEA-related rate constants because DEA is the primary source of DACT in humans.
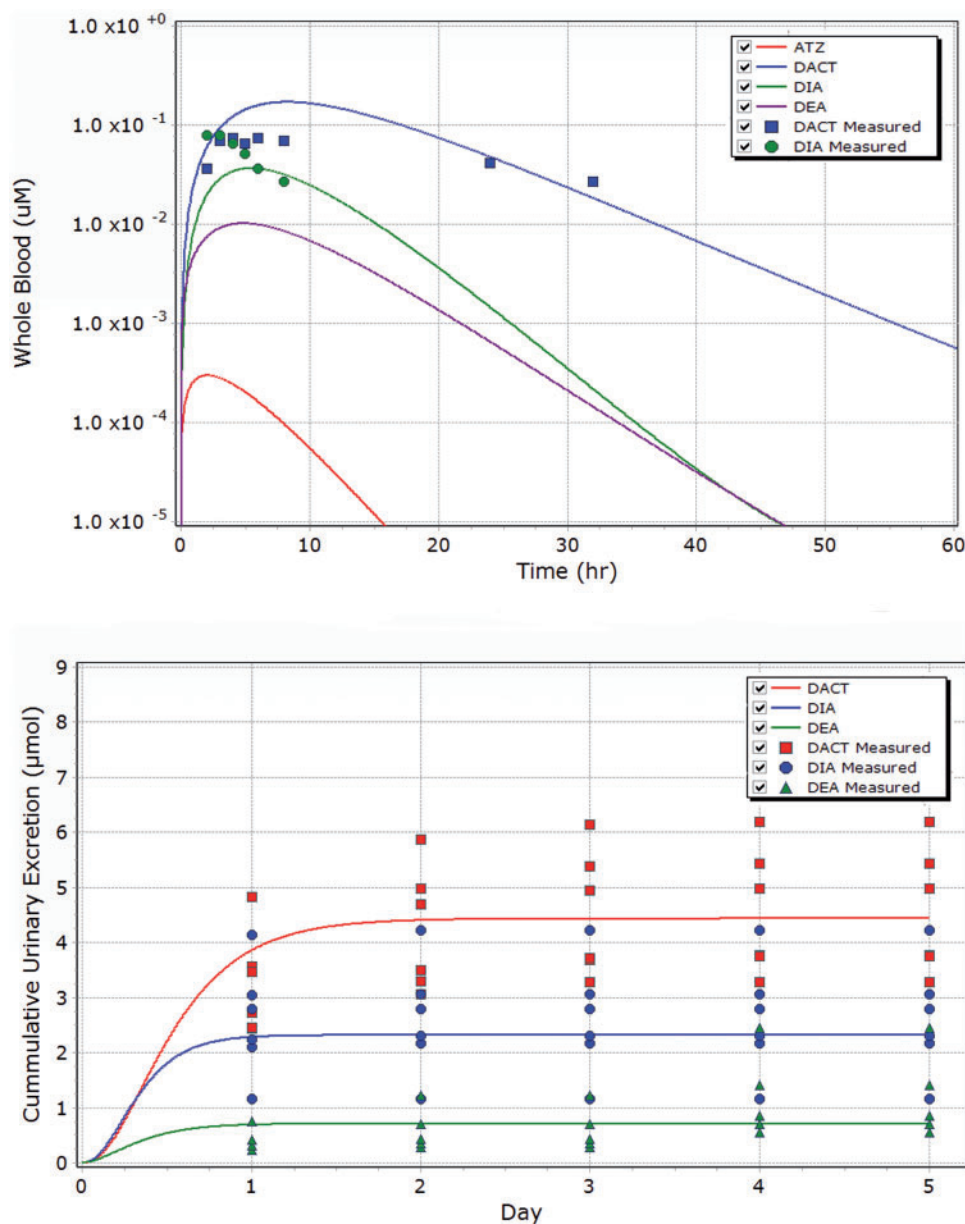
FIG. 9. Simulation of a 0.1 mg/kg oral bolus administered to humans. Top panel shows the whole blood concentration for a single individual and the bottom panel shows the cumulative urinary excretion over 5 days (points represent individual subjects).

Chlorotriazine Concentrations and the Derivation of the Biological Equivalent Dose

Plasma and urinary concentrations of ATZ, DEA, DIA, DACT, and TCT were calculated following continuous oral ATZ exposure (ie, a fractional oral dose every 0.1 h) of a 55-kg female to 1.0 µg ATZ/kg body weight/day. At steady-state, plasma concentrations were 0.00023 µg/L for ATZ, 0.0091 µg/L for DEA, 0.024 µg/L for DIA, 0.12 µg/L for DACT, and 0.21 µg/L for TCT. Concentrations in urine were 0.55, 1.44, 2.46, and 6.0 µg/L for DEA, DIA, DACT, and TCT, respectively (Table 5, Panel A). Similarly, steady-state concentrations of the chlorotriazines in plasma and urine were modeled following continuous exposure of a 55-kg adult to the ATZ POD of 1.8 mg/kg/day (Table 5, Panel B).

Biological equivalents (BE), expressed as chlorotriazine concentrations in plasma, were calculated using the approach described by Hays et al. (2011). Model predicted plasma and urine concentrations of the chlorotriazines at the POD dose were divided by a 30-fold uncertainty factor (Table 5, Panel C). A factor of three was used for animal-to-human extrapolation and a factor of 10 to describe intra-species variability. Plasma BEs were 0.014, 0.559, 1.46, and 7.01 µg/L for ATZ, DEA, DIA, and DACT, respectively (Table 5, Panel C). The BE for TCT in plasma, which was expressed as an ATZ equivalent concentration to account for differences in the molecular weights of the chlorometabolites, was 12.77 µg/L.

Average urinary BE concentrations were calculated for each chlorotriazine except ATZ (see Table 5, Panel C). The urinary excretion volume of 1.6 L/day was taken from Hays et al. (2011). Urinary BEs were 33.87, 88.17 and 146.46 µg/L for DEA, DIA and DACT, respectively. The urinary BE for TCT, expressed as the ATZ equivalent concentration, was 360.63 µg/L.

TABLE 4. Normalized Sensitivity Coefficients for Plasma and Urine Concentrations Under Steady-State Exposure Conditions

Parameter	Response Variable								
	Plasma					Urine			
	ATZ	DIA	DEA	DACT	TCT	DIA	DEA	DACT	TCT
VMAXCISO	<0.01	−0.90	−0.02	0.09	−0.03	−0.43	−0.44	0.07	−0.14
KMISO	<0.01	0.88	<0.01	−0.09	0.03	0.89	0.44	−0.10	0.26
KELIMETHYLC	<0.01	<0.01	−0.06	−0.01	−0.01	−0.44	−0.03	0.04	−0.12
VMAXCETHYL	<0.01	<0.01	−0.87	0.03	<0.01	0.02	<0.01	0.03	−0.02
KMETHYL	<0.01	<0.01	0.87	−0.03	<0.01	0.45	0.44	−0.06	0.15
PLETHYL	<0.01	<0.01	−0.06	−0.01	−0.01	<0.01	−0.03	−0.44	−0.26
KELIMDAC	<0.01	<0.01	<0.01	−0.87	−0.74	<0.01	<0.01	−0.43	<0.01
PLDA	<0.01	<0.01	<0.01	−0.87	−0.74	<0.01	0.03	−0.43	−0.26
KAOR2ATRAC	0.72	−0.05	0.15	<0.01	<0.01	−0.02	0.07	0.44	0.25
KOR1_OR2ATRAC	<0.01	<0.01	<0.01	<0.01	<0.01	<0.01	−0.07	<0.01	<0.01
KMETATRA_ISO_OR2C	−0.74	0.23	−0.74	<0.01	<0.01	0.12	−0.37	<0.01	<0.01
KMETATRA_ETHYL_OR2C	−0.19	−0.19	0.60	<0.01	<0.01	−0.21	0.67	<0.01	<0.01
KAOR2ISOC	<0.01	<0.01	<0.01	<0.01	<0.01	0.09	−0.30	<0.01	<0.01
KAOR2ETHYLC	<0.01	<0.01	<0.01	<0.01	<0.01	<0.01	<0.01	<0.01	<0.01
CLRISOC	<0.01	−0.26	0.00	−0.05	−0.07	0.37	0.37	−0.03	0.14
CLRETHYLC	<0.01	0.00	−0.25	−0.01	−0.02	<0.01	0.37	<0.01	0.03
CLRDAC	<0.01	<0.01	<0.01	−0.17	−0.15	−0.37	<0.01	0.44	0.14

TABLE 5. Concentrations of ATZ, DEA, DIA, DACT, and TCT (μg/L) in Plasma and Urine After Continuous, Steady-State Exposure of a 55-kg Female to ATZ at a Dose of 1 μg/kg (Panel A) or 1.8 mg/kg/day (Panel B), and Panel C Provides the BE Concentration (ATZ Equivalents) in Plasma and Urine After Continuous Exposure to ATZ at the POD Dose of 1.8 mg/kg/day

Chlorotriazine	Average plasma concentration (μg/L)	Average urinary[a] concentration (μg/L)
Panel A: plasma and urinary concentrations (μg/L) at ATZ dose of 1 μg/kg/day		
ATZ	0.00023	ND[b]
DIA	0.024	1.44
DEA	0.0091	0.55
DACT	0.12	2.46
TCT (ATZ Equivalents)	0.21	6.00
Panel B: plasma and urinary concentrations (μg/L) at the POD dose		
ATZ	0.42	ND[b]
DIA	43.66	2645.2
DEA	16.77	1016.0
DACT	210.19	4393.7
TCT (ATZ Equivalents)	383.12	10819.0
Panel C: BE Dose (μg/L)		
ATZ	0.014	ND[a]
DIA	1.46	88.17
DEA	0.559	33.87
DACT	7.01	146.46
TCT (ATZ equivalents)	12.77	360.63

[a]Urine volume = 1.6 L/day (Hays et al., 2011; Mage et al., 2004).
[b]The rate constant for the elimination of ATZ in urine could not be determined from the human study (Pfeil et al., 2007); the ATZ concentration was below the LOQ (5 μg/L).
Total uncertainty factor = 30; a 3× factor used to extrapolate from rat to human and a 10× factor used for intra-species variability.

DISCUSSION

The previously published PBPK model (McMullin et al., 2007a) was re-parameterized using new in vitro and in vivo data to produce a model that (1) provided more accurate estimates of the absorbed dose, and (2) reliably predicted measured plasma concentrations of the chlorotriazines in rats after gavage dosing or dietary administration. The model was scaled to man, and the clearance of DEA, DIA, and DACT from plasma into urine was calibrated against human data.

The PBPK model includes a module that allowed the input of drinking water exposure of humans to ATZ, DEA, DIA, and DACT at 30-min increments over 365 days, using an Excel-spreadsheet-based drinking water exposure calculator. The PBPK model output included the calculated plasma concentration(s) of ATZ, DIA, DEA, and/or DACT in 30-min intervals. Breckenridge et al. (2016) used these features of the human PBPK model to calculate rolling-average plasma concentrations of TCT following human exposure to chlorotriazines in drinking water, and to calculate distributions of MOEs for various toxicological PODs.

The impact of randomly drawing each of the 84 model parameters (1000 iterations) on the distribution of MOEs, derived from fixed exposure of an individual at each of the 95th and 99.9[th] percentiles of the MOE distribution, was evaluated by Breckenridge et al. (2016). The results indicated that 99% of the variability in the MOE distribution was attributable to one parameter, the rate of clearance of DACT into urine (CRLDAC). This outcome was not unexpected, because DACT's clearance rate drives both TCT peak concentration and the TCT AUC. It is likely that these dose metrics are linked to the occurrence of toxicologically relevant, adverse effects observed at high bolus doses in animal studies (Foradori et al., 2014). Even though the urinary DEA, DIA, and DACT clearance rates in this model were informed by human TCT elimination data, the model could be further improved if clearance rates for conjugated metabolites of ATZ, DEA, DIA, and DACT were available.

A kinetic study in non-human primates has been conducted, and work is underway to estimate the rate of elimination of the chlorotriazines as mercapturate and cysteine conjugates in urine (Figure 7). We expect to incorporate these additional metabolic processes into the PBPK model and to scale the non-human primate model to man. This will permit BEs to be determined for the thiol-conjugated metabolites of the

chlorotriazine. Furthermore, this new work will provide an independent validation of the existing model, by comparing model predictions based on the rodent model, scaled-to-man, to predictions obtained based on the non-human primate model, scaled-to-man.

The input module is being expanded to accept dermal and inhalation exposure data of varied durations so that risks associated with occupational or bystander exposure can be quantified. This will permit a comprehensive, rational approach for assessing aggregate and cumulative exposure to the chlorotriazines. This model could also be used to assess mixtures of chemicals that do not necessarily have the same mechanism of toxicity, but which may modulate rates of metabolism or clearance of chemicals belonging to common mechanism groups.

Overall, the re-parameterized PBPK model for the chlorotriazines is a useful tool for (1) predicting steady-state, plasma or urinary concentrations of ATZ, DEA, DIA, DACT, and TCT following exposure of humans to known doses of the chlorotriazines, (2) back-calculating the human dose from measured plasma or urinary concentrations (Clewell et al., 2008), and (3) for calculating the BE for TCT at the POD. The model has been used successfully to convert temporally fluctuating exposure to the chlorotriazines in drinking water into internal TCT plasma concentrations, as well as to assess the risk of such exposure by calculating MOE distributions (Breckenridge et al., 2016). It is expected that as more becomes known about the molecular processes underlying the effects of the chlorotriazines (Foradori et al., 2013, 2014), pharmacokinetic models, like the one presented in this article, will be combined with response-dynamic models to achieve a deeper understanding of adverse outcome pathways.

Funding

SUPPLEMENTARY DATA

Supplementary data are available online at http://toxsci.oxfordjournals.org/.

REFERENCES

Adami, H. O., Berry, S. C., Breckenridge, C. B., Smith, L. L., Swenberg, J. A., Trichopoulos, D., Weiss, N. S., and Pastoor, T. P. (2011). Toxicology and epidemiology: Improving the science with a framework for combining toxicological and epidemiological evidence to establish causal inference. *Toxicol. Sci.* **122**, 223–234.

Ashby, J., Tinwell, H., Stevens, J., Pastoor, T., and Breckenridge, C. B. (2002). The effects of atrazine on the sexual maturation of female rats. *Regul. Toxicol. Pharmacol.* **35**, 468–473.

Barr, D. B., Panuwet, P., Nguyen, J. V., Udunka, S., and Needham, L. L. (2007). Assessing exposure to atrazine and its metabolites using biomonitoring. *Environ. Health Perspect.* **115**, 1474–1478.

Breckenridge, C. B., Campbell, J. L., Clewell, H. J., 3rd, Anderson, M. E., Valdez-Flores, C., and Sielken, R. L., Jr. (2016). PBPK-Based Probabilistic Risk Assessment for Total Chlorotriazines in Drinking Water. *Toxicol. Sci.* **150**, 269–282.

Breckenridge, C. B., Sawhney Coder, P., Tisdel, M. O., Simpkins, J. W., Yi, K. D., Foradori, C. D., and Handa, R. J. (2015). Effect of age, duration of exposure, and dose of atrazine on sexual maturation and the luteinizing hormone surge in the female Sprague-Dawley rat. *Birth Defects Res. B Dev. Reprod. Toxicol.* **104**, 204–217.

Bridges, D. C. (2008). *Benefits of Triazine Herbicides in Corn and Sorghum Production* (H. M. LeBaron, J. E. McFarland, and O. C. Burnside, Eds.), pp. 163–174. Elsevier, San Diego. doi: 10.1016/B978-044451167-6.50016-7.

Brown, R. P., Delp, M. D., Lindstedt, S. L., Rhomberg, L. R., and Beliles, R. P. (1997). Physiological parameter values for physiologically based pharmacokinetic models. *Toxicol. Ind. Health* **13**, 407–484.

Chevrier, C., Limon, G., Monfort, C., Rouget, F., Garlantezec, R., Petit, C., Durand, G., and Cordier, S. (2011). Urinary biomarkers of prenatal atrazine exposure and adverse birth outcomes in the PELAGIE Birth Cohort. *Environ. Health Perspect.* **119**, 1034–1041.

Chevrier, C., Serrano, T., Lecerf, R., Limon, G., Petit, C., Monfort, C., Hubert-Moy, L., Durand, G., and Cordier, S. (2014). Environmental determinants of the urinary concentrations of herbicides during pregnancy: The PELAGIE mother–child cohort (France). *Environ. Int.* **63**, 11–18.

Clewell, H. J., Tan, Y. M., Campbell, J. L., and Andersen, M. E. (2008). Quantitative interpretation of human biomonitoring data. *Toxicol. Appl. Pharmacol.* **231**, 122–133.

Dooley, G. P., Hanneman, W. H., Carbone, D. L., Legare, M. E., Andersen, M. E., and Tessari, J. D. (2007). Development of an immunochemical detection method for atrazine-induced albumin adducts. *Chem. Res. Toxicol.* **20**, 1061–1066.

Foradori, C. D., Sawhney Coder, P., Tisdel, M., Yi, K. D., Simpkins, J. W., Handa, R. J., and Breckenridge, C. B. (2014). The effect of atrazine administered by gavage or in diet on the LH surge and reproductive performance in intact female Sprague-Dawley and Long Evans rats. *Birth Defects Res. B Dev. Reprod. Toxicol.* **101**, 262–275.

Foradori, C. D., Zimmerman, A. D., Hinds, L. R., Zuloaga, K. L., Breckenridge, C. B., and Handa, R. J. (2013). Atrazine inhibits pulsatile gonadotropin-releasing hormone (GnRH) release without altering GnRH messenger RNA or protein levels in the female rat. *Biol. Reprod.* **88**, 9/1–9/7.

Goodman, M., Mandel, J. S., DeSesso, J. M., and Scialli, A. R. (2014). Atrazine and pregnancy outcomes: A systematic review of epidemiologic evidence. *Birth Defects Res. B Dev. Reprod. Toxicol.* **101**, 215–236.

Hays, S. M., Aylward, L. L., Kirman, C. R., Krishnan, K., and Nong, A. (2011). Biomonitoring equivalents for di-isononyl phthalate (DINP). *Regul. Toxicol. Pharmacol.* **60**, 181–188.

ICRP (2002). Basic anatomical and physiological data for use in radiological protection: Reference values. A report of age- and gender-related differences in the anatomical and physiological characteristics of reference individuals. ICRP Publication 89. *Ann. ICRP* **32**, 5–265.

Jablonkai, I., and Hatzios, K. K. (1993). *In Vitro* conjugation of chloroacetanilide herbicides and atrazine with thiols and contribution of nonenzymatic conjugation to their glutathione-mediated metabolism in corn. *J. Agric. Food Chem.* **41**, 1736–1742.

Koolschijn, P. C., van Haren, N. E., Hulshoff Pol, H. E., and Kahn, R. S. (2008). Hypothalamus volume in twin pairs discordant for schizophrenia. *Eur. Neuropsychopharmacol.* **18**, 312–315.

Laws, S. C., Ferrell, J. M., Stoker, T. E., and Cooper, R. L. (2003). Pubertal development in female Wistar rats following exposure to propazine and atrazine biotransformation by-products, diamino-S-chlorotriazine and hydroxyatrazine. *Toxicol. Sci.* **76**, 190–200.

Laws, S. C., Ferrell, J. M., Stoker, T. E., Schmid, J., and Cooper, R. L. (2000). The effects of atrazine on female Wistar rats: An evaluation of the protocol for assessing pubertal development and thyroid function. *Toxicol. Sci.* **58**, 366–376.

Mage, D. T., Allen, R. H., Gondy, G., Smith, W., Barr, D. B., and Needham, L. L. (2004). Estimating pesticide dose from urinary pesticide concentration data by creatinine correction in the third National Health and Nutrition Examination Survey (NHANES-III). *J. Expo. Anal. Environ. Epidemiol.* **14**, 457–465.

McMullin, T. S., Andersen, M. E., Tessari, J. D., Cranmer, B., and Hanneman, W. H. (2007a). Estimating constants for metabolism of atrazine in freshly isolated rat hepatocytes by kinetic modeling. *Toxicol. in vitro* **21**, 492–501.

McMullin, T. S., Brzezicki, J. M., Cranmer, B. K., Tessari, J. D., and Andersen, M. E. (2003). Pharmacokinetic modeling of disposition and time-course studies with [14C]atrazine. *J. Toxicol. Environ. Health A* **66**, 941–964.

McMullin, T. S., Hanneman, W. H., Cranmer, B. K., Tessari, J. D., and Andersen, M. E. (2007b). Oral absorption and oxidative metabolism of atrazine in rats evaluated by physiological modeling approaches. *Toxicology* **240**, 1–14.

O'Flaherty, E. J., Scott, W., Schreiner, C., and Beliles, R. P. (1992). A physiologically based kinetic model of rat and mouse gestation: Disposition of a weak acid. *Toxicol. Appl. Pharmacol.* **112**, 245–256.

Pfeil, R., Dellarco, V., and Davies, L. (2007). ATRAZINE. In Pesticide residues in food——2007: Toxicological evaluations. Joint FAO/WHO Meeting on Pesticide Residues: Report of the Joint Meeting of the FAO Panel of Experts on Pesticide Residues in Food and the Environment and the WHO Core Assessment Group on Pesticide Residues, Geneva, Switzerland, 18–27 September 2007, pp. 37–138. World Health Organization [u.a.], Rome.

Sohlenius-Sternbeck, A. K. (2006). Determination of the hepato-cellularity number for human, dog, rabbit, rat and mouse livers from protein concentration measurements. *Toxicol. In Vitro* **20**, 1582–1586.

Stoker, T. E., Guidici, D. L., McElroy, W. K., Laws, S. C., and Cooper, R. L. (2000). The effect of atrazine (ATR) on puberty in male Wistar rats. *Toxicologist* **54**, 366.

Thede, B. (1987). *Study of [14C] Atrazine Dose/Response Relationship in the Rat*, pp. 33. Syngenta Crop Protection, LLC, Internal Report. Greensboro, NC.

Tierney, D. P., Christensen, B. R., Dando, C., and Marut, K. M. (2008). *Atrazine and Simazine Monitoring Data in Community Water Systems in the United States during 1993 to 2000* (H. M. LeBaron, J. E. McFarland, and O. C. Burnside, Eds.), pp. 439–449. Elsevier, San Diego. doi: 10.1016/B978-044451167-6.50032-5.

Timchalk, C., Dryzga, M. D., Langvardt, P. W., Kastl, P. E., and Osborne, D. W. (1990). Determination of the effect of tridiphane on the pharmacokinetics of [14C]-atrazine following oral administration to male Fischer 344 rats. *Toxicology* **61**, 27–40.

Tremblay, R. T., Kim, D., and Fisher, J. W. (2012). Determination of tissue to blood partition coefficients for nonvolatile herbicides, insecticides, and fungicides using negligible depletion solid-phase microextraction (nd-SPME) and ultrafiltration. *J. Toxicol. Environ. Health A* **75**, 288–298.

USEPA (2002). *The Grouping of a Series of Triazine Pesticides Based on a Common Mechanism of Toxicity*. United States Environmental Protection Agency, Office of Pesticide Programs, Health Effects Division, Washington, DC. Available at: http://www.regulations.gov/#!documentDetail;D=EPA-HQ-OPP-2005-0481-0011, Accessed February 2, 2016.

USEPA (2006). *Cumulative Risk from Triazine Pesticides*, pp. 67. U.S. Environmental Protection Agency, Office of Pesticide Programs, Health Effects Division. Washington, DC.